

Adaptive Hit or Miss Transform

Vladimir Ćurić¹, Sébastien Lefèvre², and Cris L. Luengo Hendriks³

¹ Department of Cell and Molecular Biology, Uppsala University, Uppsala, Sweden
`vladimir.curic@icm.uu.se`

² Univ. Bretagne-Sud, IRISA, Vannes, France
`sebastien.lefevre@irisa.fr`

³ Centre for Image Analysis, Uppsala University, Uppsala, Sweden
`cris@cb.uu.se`

Abstract. The Hit or Miss Transform is a fundamental morphological operator, and can be used for template matching. In this paper, we present a framework for adaptive Hit or Miss Transform, where structuring elements are adaptive with respect to the input image itself. We illustrate the difference between the new adaptive Hit or Miss Transform and the classical Hit or Miss Transform. As an example of its usefulness, we show how the new adaptive Hit or Miss Transform can detect particles in single molecule imaging.

Keywords: Hit or Miss Transform, adaptive morphology, adaptive structuring elements, template matching.

1 Introduction

At its early development, mathematical morphology was dedicated to binary images using the notion of structuring element [1–3]. A structuring element was a fixed shape used to probe every point in the image. Morphological operators defined with these fixed structuring elements are still very commonly used for many different problems in image analysis. Nevertheless, the basic morphological operators can be extended to adaptive morphological operators using adaptive structuring elements, which are structuring elements that change size and shape according to local characteristics of the image. The construction of different adaptive structuring elements and consequently adaptive morphological operators has attracted a lot of attention in the last decade [4–10]. Theoretical advances and limitations of adaptive mathematical morphology have been explored by several researchers [11–14]. Adaptivity can be included into morphological operators in different ways [15], and the recent overview paper on adaptive mathematical morphology presents a comparison of different methods for adaptive structuring elements [16].

Despite adaptive mathematical morphology has been developed extensively in the last decade, its development is mostly based on the construction of new types of adaptive structuring elements. These structuring elements are then applied to basic morphological operators (erosions, dilations, openings and closings)

or noise filtering techniques. More complex operators or filters have not been extensively studied. In this paper, we focus on one such operator, the Hit or Miss Transform (HMT).

The HMT has most often been used for detecting a given pattern in a binary image (this problem is also called template matching) and has a number of different applications [17–19]. Two survey papers on HMT have been presented recently [20, 21]. HMT relies on a pair of disjoint structuring elements, where one fits the foreground (object) and the other fits the background. The common approach to ensure robustness to variations in the shape or size of the sought pattern is to consider a set of structuring element pairs; a match is allowed if one of the pairs match the considered pattern [17]. Instead of using a limited, pre-defined set of structuring element pairs, we propose to use a single adaptive structuring element pair in order to limit the computation burden.

In this paper, we propose a framework for adaptive Hit or Miss Transform, where the HMT is defined for gray level images using the notion of adaptive structuring elements. We present a way to define the adaptive HMT, and experimentally show its advantages over the classical HMT (i.e. with fixed structuring elements). In the rest of this paper, we will denote as *classical HMT* the HMT defined using fixed structuring elements, and as *adaptive HMT* the HMT defined using adaptive structuring elements. In addition, we illustrate the usefulness of adaptive HMT to a real life imaging problem, i.e. finding fluorescent dots in single molecule imaging.

2 Background

In this section, we recall the basics of HMT and adaptive mathematical morphology with adequate definitions and notations. First, we present the HMT for binary images as well as its extension to gray level images. Second, we recall the main concepts of adaptive mathematical morphology and briefly present the method for adaptive structuring elements that will be used in this paper.

2.1 Hit or Miss Transform

The Hit or Miss Transform aims to extract objects (i.e. parts of the image) that fit two distinct criteria. These criteria are defined as structuring elements that are respectively associated with foreground (object) and background. Several equivalent formulations have been given to define the HMT, and we use the following one to denote the HMT of an image I by the couple of structuring elements (SE_O, SE_B) :

$$\text{HMT}_{SE_O, SE_B}(I) = \varepsilon_{SE_O}(I) \setminus \delta_{SE_B'}(I), \quad (1)$$

where $\varepsilon_{SE_O}(I)$ and $\delta_{SE_B}(I)$ represent erosion and dilation of I with structuring elements SE_O and SE_B respectively, and $A' : x \rightarrow -x$ denotes the reflexion of the structuring element A with respect to the its origin.

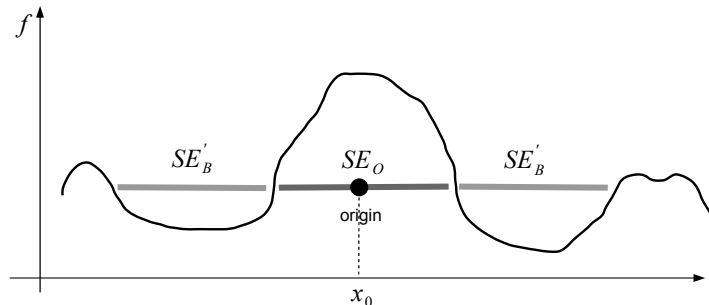


Fig. 1. Example of 1D function f where SE_O fits the region (foreground) around the point x_0 and SE'_B fits the neighbourhood (background) of the same point.

Conversely to the binary case, various non equivalent definitions have been given for the gray scale HMT. The reader will find in [22] a common theoretical framework, and in [20] a review of these existing works. In this paper, and for the sake of illustration, we will consider the definition from Soille [23] assuming flat structuring elements (see Fig. 1), i.e.,

$$\text{HMT}_{SE_O, SE'_B}(I)(x) = \max \{ \varepsilon_{SE_O}(I)(x) - \delta_{SE'_B}(I)(x), 0 \}, \quad x \in D \quad (2)$$

where D is the image domain.

Let us note, however, that nothing prevents the method proposed in this paper to be applied to other HMT definitions, including those that are dealing with structuring functions, since adaptive structuring functions have been explored before [24, 25].

2.2 Adaptive Structuring Elements

As mentioned in the introduction, adaptive mathematical morphology has attracted a lot of attention in recent years and is a topic of ongoing research. Adaptive structuring elements adapt to the image structures by taking into account different image attributes such as gray level values, geodesic distances between points in the image, the image gradient, the Hessian, etc. There exist many ways to include these information in the construction of adaptive structuring elements, and hence there exist many different methods to construct adaptive structuring elements [16].

Any of these existing methods could be used to define an adaptive HMT. However, for the sake of illustration, we will use adaptive structuring elements that have a fixed shape and varying size [26]. We have chosen these adaptive structuring elements since they can be computed in linear time with respect to the number of pixels in the image. The size of the structuring element is adjusted using the salience map SM.

The salience map SM is computed from the salience distance transform [27] of the edge image, where edges are weighted according to their importance, i.e.,

saliency, containing information about the important structures in the image. To preserve most of the edges in the image, we use the gradient estimation and non-maximal suppression from the Canny edge detector [28]. To compute the non-maximal suppression, we use Gaussian derivatives to estimate the gradient in the input image, but exclude the hysteresis thresholding from the Canny edge detector. This approach preserves even the edges with a small response in the gradient image. Formally, $\text{NMS}(f)$ is the image obtained by computing the gradient magnitude and non-maximal suppression of the input image f . The edge pixels are initialized with the negative values of their saliency and the non-edge pixels are set to infinity [27]. The saliency distance transform is computed with the classical two-pass chamfering algorithm [29]. After the saliency distance transform is propagated from $-\text{NMS}(f)$, the distance image is offset to all positive values. Then, by inverting these values, we obtain the saliency map $\text{SM}(f)$, which can be formally written as

$$[\text{SM}(f)](y) = \text{Offset} + \bigvee_{x \in D} \left(\text{NMS}(f)(x) - d(x, y) \right), \quad y \in D, \quad (3)$$

where

$$\text{Offset} = \bigwedge_{y \in D} \bigvee_{x \in D} \left(\text{NMS}(f)(x) - d(x, y) \right), \quad (4)$$

and $d(x, y)$ is a spatial distance.

This saliency map SM contains the information about the spatial distance between points in the image and preserves the information about the saliency of the edges in the image, where the largest values in the saliency map SM correspond to the strongest edges and lower values to weaker ones, and its value decreases with the distance to the edges in the image [9].

In this paper, we consider adaptive structuring elements that preserve better strong edges than weak ones [26]. We find the value of the largest local maximum of SM , and the value of its largest local minimum, denoted here with M and m respectively. Then, the size (radius) of the adaptive structuring element is defined by

$$r(x) = \left\lfloor \left| \text{SM}(x) - \frac{m + M}{2} \right| \cdot c \right\rfloor, \quad \text{for all } x \in D, \quad (5)$$

where c is a constant that additionally adjusts the size of the structuring elements.

3 Method

The selection of appropriate structuring elements determines the performance of the HMT and its applications to template matching. Template matching using the HMT is often not trivial for the case of binary images, and it is even more complicated for gray level images [17].

A specific object in the image can be extracted using the HMT with two structuring elements: one defines the object and another defines what is not the

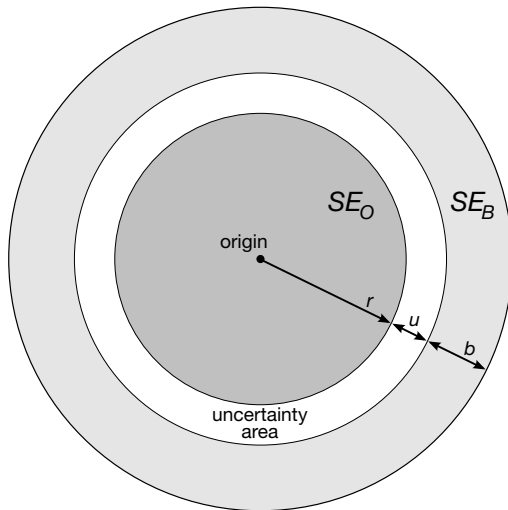


Fig. 2. Example of structuring elements SE_O , SE_B used for the extraction of objects.

object (the object’s surrounding, or often called background). Here, the following steps are necessary:

1. The structuring element representing the object is fully defined (SE_O), as well as the structuring element dedicated to background (SE_B).
2. HMT is defined using adaptive structuring elements that depend on the object and its properties. In order to be able to match the object even with discretization artefacts (e.g., stairing effect), it might be necessary to define an uncertainty area located between the two structuring elements [30] (see Fig. 2).

In this paper, we consider the adaptive structuring elements such that the size of adaptive structuring elements SE_O and SE_B is defined in the following way (see Fig. 2)

$$SE_O(x) = \{y \in D : |x - y| < r(x)\} \quad (6)$$

$$SE_B(x) = \{y \in D : r(x) + u \leq |x - y| < r(x) + u + b\} \quad (7)$$

where the adaptive radius $r(x)$, $x \in D$ is computed using the definition by Eq. (5), and u and b define the size of the uncertainty area and the size of the background area, respectively.

Note that, in this paper, we keep the uncertainty area u and the background b fixed for all points in the image. These two parameters that determine the position and size of the background structuring element SE_B can also have different values dependent on the image. We feel that selection of these parameters issue deserves further studies, and therefore is placed high on our list of future work.

4 Experiments and Results

Three experiments have been conducted to test the proposed method for adaptive HMT. While the first one considers a synthetic image of circular shapes with different sizes and image contrasts, the two latter deal with microscopy images of single molecules in bacteria cells. For all performed experiments, adaptive structuring elements are the Euclidean disks with adaptive radius computed by Eq. (5).

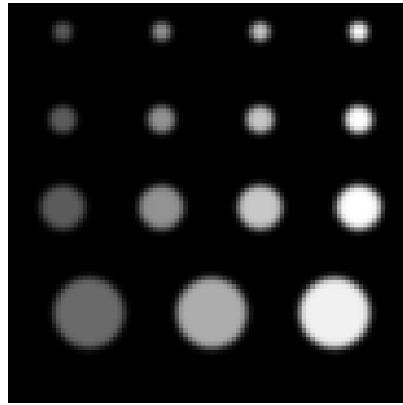
In the first experiment (Experiment 1), we consider an image of disks of different sizes and contrasts, where the shapes in each row have the same size and different contrast (see Fig. 3(a)). We examine the performance of the adaptive HMT and compare it with performance of the classical HMT. For the comparison, we defined the radius of the fixed structuring element pair as the mean radius of the adaptive structuring elements pair over the whole image, i.e., the size of the fixed structuring elements is assigned to $\text{mean}\{r(x) : x \in D\}$.

The adaptive HMT treats differently objects that have the same size but different contrast, which is not the case for the classical HMT, as depicted in Fig. 3. While the latter finds objects of the same size (Fig. 3(b) and (c)), the former detects object with respect to their contrast and not their size (Fig. 3(d) and (e)).

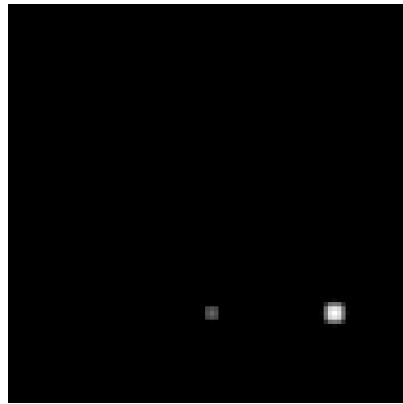
In the next two experiments (Experiment 2 and 3), we consider a realistic use of adaptive HMT dealing with microscopy images of the single molecules in living cells, in particular in bacteria E-coli (see Figs. 4 and 5). Single molecules appear visible as fluorescent dots and are brighter than the very noisy inhomogeneous background. For live cell imaging, for which fluorescence microscopy is often used, the signal-to-noise ratio (SNR) is often very low, making automated spot detection a very challenging task [31]. Also, since these are images of single molecules, fluorescent spots are only a few nanometers wide; however, due to diffraction limit, they appear as spots that cover a few pixels.

In Experiment 2, we examine how the size of adaptive structuring elements influences the performance of adaptive HMT. We use an adaptive structuring element defined by Eq. (5), and consider different values for the constant c that determines the size of the adaptive structuring element. For this experiment, we have no uncertainty region between two structuring elements SE_O and SE_B , i.e. $u = 0$. Also, we keep the size of the background structuring element SE_B fixed with $b = 3$. The results are shown in Fig. 4. Despite the fact that ground truth does not exist for these data, it is obvious that the two fluorescent dots can be found in the presented image (see Fig. 4(a)): one of them is close to the top edge of the image, the other is near the middle. These two fluorescent dots are only found when $c = 0.1$ (Fig. 4(b)), while for larger c the dimmer of the two fluorescent dots cannot be found (see Fig. 4(c) and (d)). In contrast, for the classical HMT there is no parameter setting that allows it to find both dots simultaneously.

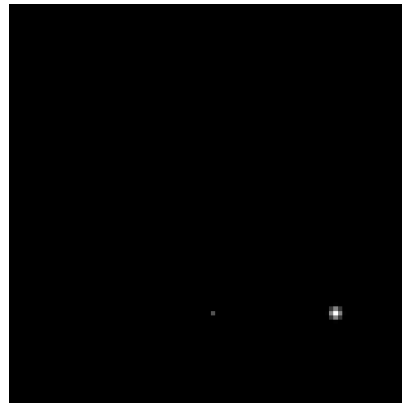
In Experiment 3, we investigate how the selection of the background structuring element SE_B influences the adaptive HMT. We vary the size of the uncertainty region, which is the region between the foreground structuring element



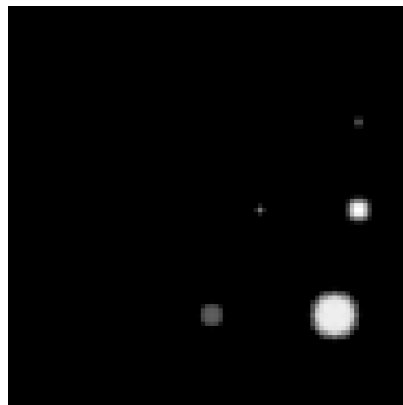
(a)



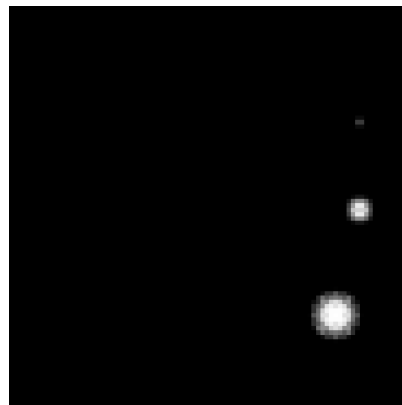
(b)



(c)



(d)



(e)

Fig. 3. Comparison between the classical HMT and adaptive HMT using different radii $r(x)$, and for $u = 2$ and $b = 1$. The radius of fixed structuring element is equal to $\text{mean}\{r(x) : x \in D\}$. (a) Input image; (b) Classical HMT that is compared to the adaptive HMT in (d); (c) Classical HMT that is compared to the adaptive HMT in (e); (d) Adaptive HMT with $c = 0.2$; (e) Adaptive HMT with $c = 0.4$.

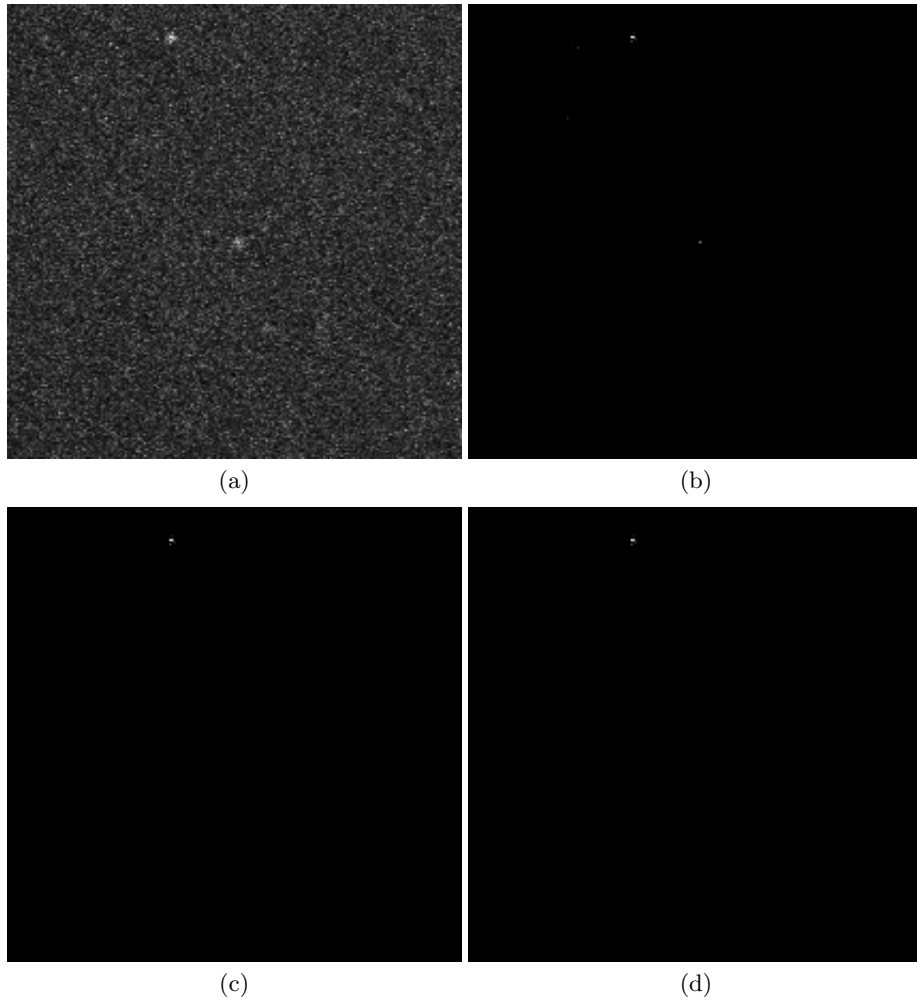


Fig. 4. Adaptive HMT for $u = 0$ and $b = 3$, with various values for size parameter c . (a) Input image; (b) Adaptive HMT, $c = 0.1$; (c) Adaptive HMT, $c = 0.5$; (d) Adaptive HMT, $c = 1$. Note that the classical HMT can find at most one dot at the time.

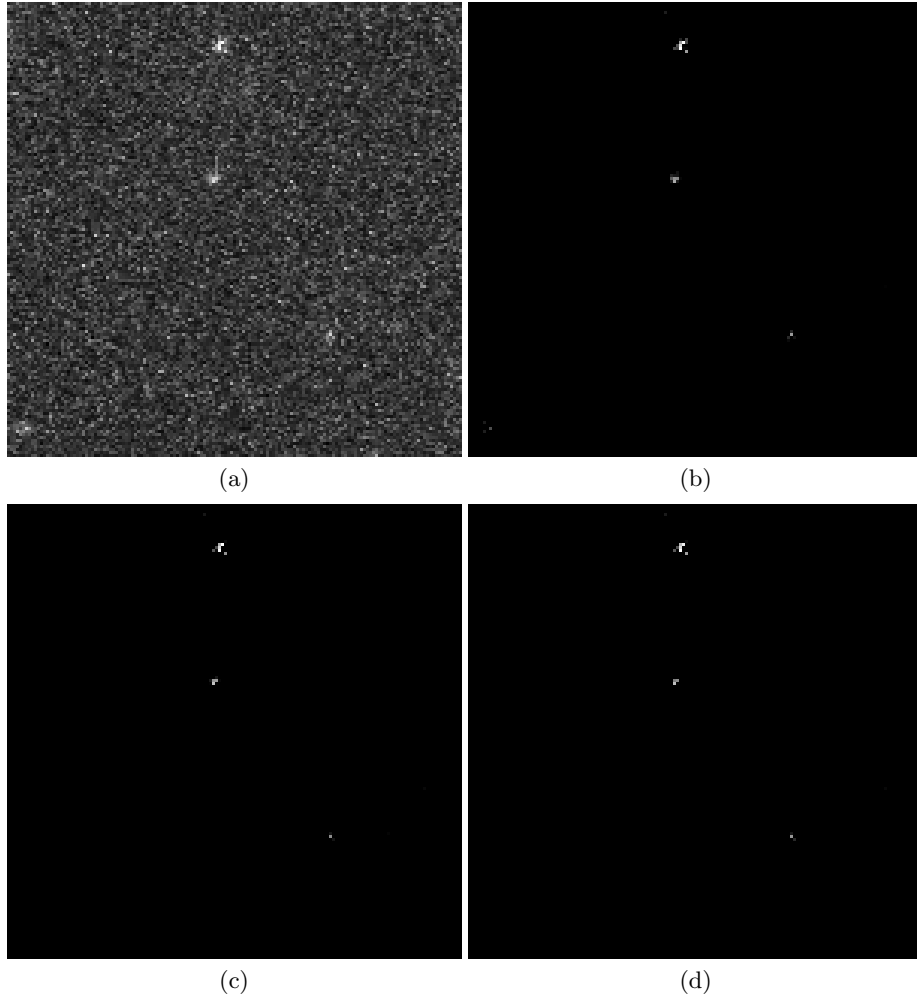


Fig. 5. Adaptive HMT for different sizes of the uncertainty region between structuring elements SE_O and SE_B , i.e., for different values of u . Here, $c = 0.1$ and $b = 2$; (a) Input image; (b) Adaptive HMT, $u = 1$; (c) Adaptive HMT, $u = 2$; (d) Adaptive HMT, $u = 3$. Note that the classical HMT can find at most one dot at the time.

SE_O and the background structuring element SE_B (see Fig. 2). The size and shape of the uncertainty region determines how far SE_O and SE_B will be apart from each other, and it can significantly influence the result of HMT, as this region gives the operator flexibility to accept more objects. For this experiment, we fixed $c = 0.5$, and vary u and b , which define the uncertainty region and the background structuring element SE_B . Out of the four fluorescent dots in the image, three were detected in all three cases, whereas the fourth was detected only with a small uncertainty region.

We can conclude that besides the background and foreground size parameters c and b , the width of the uncertainty area u also impacts the properties of the pair of adaptive structure elements (foreground, background) and thus the result of the adaptive HMT. Similarly to any template matching solution, these three parameters are context-dependent and need to be set depending on the application considered.

5 Summary and Conclusions

We have proposed the Hit or Miss Transform (HMT) that is defined with an adaptive structuring element pair. We used adaptive structuring elements based on the salience information in the image [26]. Nevertheless, any other method for adaptive structuring elements can be used. Our approach uses an isotropic structuring element that scales with the distance to and strength of edges in the image. Closer to a strong edge, the structuring element is smaller. The result is an adaptive HMT that detects small, bright objects, and larger, dimmer objects at the same time. This operator, in contrast to the classical HMT, does not detect objects based on size and shape alone, but at the same time includes information of their contrast.

We have presented an application for the adaptive HMT operator in the context of template matching, illustrating the usefulness of such an operator. Experiments on both synthetic and real images show that the adaptive HMT outperforms the classical HMT with fixed structuring elements. The results obtained on microscopy images illustrated the potential of this new operator.

Our approach to adaptive HMT requires the definition of three constants: r scales the object structuring element, b scales the background structuring element, and u scales the uncertainty area, the space in between the two structuring elements. The best values for these three parameters are application dependent.

We have used Soille’s definition for gray scale HMT [23]. There exist other definitions for gray scale HMT in the literature and we plan to explore these other definitions, as well as alternative methods for adapting the structuring elements. We are also thinking about how to apply the adaptive HMT to color and multivariate images.

Acknowledgements

The images used in Figs. 4 and 5 are courtesy of Prof. Johan Elf, Department of Cell and Molecular Biology, Uppsala University, Sweden.

This work has been initiated when Vladimir Ćurić and Cris L. Luengo Hendriks visited IRISA/Univ. Bretagne-Sud, with mobility grants from Univ. Bretagne-Sud and French Embassy in Sweden (FRÖ program) respectively.

References

1. Matheron, G.: Random sets and integral geometry. Willey, New York (1975)
2. Serra, J.: Image analysis and mathematical morphology. Academic Press, London (1982)
3. Serra, J.: Image analysis and mathematical morphology, vol. 2: Theoretical advances. Academic Press, New York (1988)
4. Lerallut, R., Decencière, E., Meyer, F.: Image filtering using morphological amoebas. *Image and Vision Computing* **25**(4) (2007) 395–404
5. Debayle, J., Pinoli, J.: General adaptive neighborhood image processing – part I: Introduction and theoretical aspects. *Journal of Mathematical Imaging and Vision* **25**(2) (2006) 245–266
6. Tankyevych, O., Talbot, H., Dokládal, P.: Curvilinear morpho-Hessian filter. In *Proc. of IEEE International Symposium on Biomedical Imaging: From Nano to Macro* (2008) 1011–1014
7. Angulo, J., Velasco-Forero, S.: Structurally adaptive mathematical morphology based on nonlinear scale-space decompositions. *Image Analysis & Stereology* **30**(2) (2011) 111–122
8. Verdú-Monedero, R., Angulo, J., Serra, J.: Anisotropic morphological filters with spatially-variant structuring elements based on image-dependent gradient fields. *IEEE Transactions on Image Processing* **20**(1) (2011) 200–212
9. Ćurić, V., Luengo Hendriks, C.L., Borgefors, G.: Saliency adaptive structuring elements. *IEEE Journal of Selected Topics in Signal Processing* **6**(7) (2012) 809–819
10. Landström, A., Thurley, M.J.: Adaptive morphology using tensor-based elliptical structuring elements. *Pattern Recognition Letters* **34**(12) (2013) 1416–1422
11. Roerdink, J.B.T.M.: Adaptive and group invariance in mathematical morphology. In *Proc. of IEEE International Conference on Image Processing* (2009) 2253–2256
12. Bouaynaya, N., Charif-Chefchaoui, M., Schonfeld, D.: Theoretical foundations of spatially-variant mathematical morphology part I: Binary images. *IEEE Transactions on Pattern Analysis and Machine Intelligence* **30**(5) (2008) 823–836
13. Bouaynaya, N., Schonfeld, D.: Theoretical foundations of spatially-variant mathematical morphology part II: Gray-level images. *IEEE Transactions on Pattern Analysis and Machine Intelligence* **30**(5) (2008) 837–850
14. Velasco-Forero, S., Angulo, J.: On nonlocal mathematical morphology. In: *Proceedings of the International Symposium on Mathematical Morphology*, Springer (2013) 219–230
15. Maragos, P., Vachier, C.: Overview of adaptive morphology: Trends and perspectives. In: *Proceedings of the International Conference on Image Processing*, IEEE (2009) 2241–2244

16. Ćurić, V., Landström, A., Thurley, M.J., Luengo Hendriks, C.L.: Adaptive mathematical morphology – A survey of the field. *Pattern Recognition Letters* **47** (2014) 18–28
17. Perret, B., Lefèvre, S., Collet, C.: A robust hit-or-miss transform for template matching applied to very noisy astronomical images. *Pattern Recognition* **42**(11) (2009) 2470–2480
18. Weber, J., Tabbone, S.: Symbol spotting for technical documents: An efficient template-matching approach. In: *Proceedings of the IEEE International Conference on Pattern Recognition*. (2012) 669–672
19. Lefèvre, S., Weber, J.: Automatic building extraction in VHR images using advanced morphological operators. In: *Proceedings of the Urban Remote Sensing Joint Event, IEEE* (2007) 1–5
20. Murray, P., Marshall, S.: A review of recent advances in the hit-or-miss transform. *Advances in imaging and electron physics* **175** (2012) 221–282
21. Lefèvre, S., Aptoula, E., Perret, B., Weber, J.: Morphological template matching in color images. In: *Advances in Low-Level Color Image Processing*. Springer Netherlands (2014) 241–277
22. Naegel, B., Passat, N., Ronse, C.: Grey-level hit-or-miss transforms – part I: Unified theory. *Pattern Recognition* **40**(2) (2007) 635–647
23. Soille, P.: Advances in the analysis of topographic features on discrete images. In: *Proceedings of the 10th International Conference on Discrete Geometry for Computer Imagery*. (2002) 175–186
24. Angulo, J.: Morphological bilateral filtering and spatially-variant adaptive structuring functions. In: *Proceedings of the International Symposium on Mathematical Morphology*, Springer (2011) 212–223
25. Ćurić, V., Luengo Hendriks, C.L.: Saliency-based parabolic structuring functions. In: *Proceedings of the 11th International Symposium on Mathematical Morphology*. Springer (2013) 183–194
26. Ćurić, V., Luengo Hendriks, C.L.: Adaptive structuring elements based on saliency information. In: *Proceedings of the International Conference on Computer Vision and Graphics*. (2012) 321–328
27. Rosin, P., West, G.: Saliency distance transforms. *Graphical Models and Image Processing* **57**(6) (1995) 483–521
28. Canny, J.: A computational approach to edge detection. *IEEE Transactions on Pattern Analysis and Machine Intelligence*, (6) (1986) 679–698
29. Borgefors, G.: Distance transformations in digital images. *Computer Vision, Graphics, and Image Processing* **34**(3) (1986) 344–371
30. Weber, J., Lefèvre, S.: Spatial and spectral morphological template matching. *Image and Vision Computing* **30**(12) (2012) 934–945
31. Smal, I., Loog, M., Niessen, W., Meijering, E.: Quantitative comparison of spot detection methods in fluorescence microscopy. *IEEE Transactions on Medical Imaging* **29**(2) (2010) 282–301